Top-electrode and roughening effects in electron tunnelling spectroscopy

1989 J. Phys.: Condens. Matter 1 1107

(http://iopscience.iop.org/0953-8984/1/6/009)

J. Phys.: Condens. Matter **1** (1989) 1107–1118. Printed in the UK

Top-electrode and roughening effects in electron tunnelling spectroscopy

A K Sleigh, M E Taylor, C J Adkins and W A Phillips
Cavendish Laboratory, Madingley Road, Cambridge CB3 0HE, UK

Received 13 September 1988, in final form 24 October 1988

Abstract. The variation in intensity of molecular peaks in inelastic tunnelling spectra of formate-doped Al–alumina–metal tunnel junctions has been studied for a range of top electrodes and for a series of junctions roughened by prior deposition of CaF_2 films of varying thickness. Intensities were found to decrease for different top electrodes in the order Pb, Ag, Au, Sn, In, Cu and Al, the last giving no measurable spectra, and to decrease with increasing junction roughness in the case of Pb. These results are successfully and coherently interpreted in terms of a detailed model of the metal–formate–alumina interface. This model takes into account the structure of the alumina, the packing of formate ions, and the interfacial and surface energies which, together with size, determine the structure of the top metal electrode at the interface.

1. Introduction

Inelastic electron tunnelling spectroscopy (IETS) is a powerful and well established technique for the study of vibrational excitations in metal–insulator–metal structures including, in particular, those of molecular species incorporated in the barrier (Hansma 1982, Adkins and Phillips 1985, Sleigh *et al* 1986). A mode of energy $\hbar\omega$ is detected as a small step in the differential conductance of the tunnel junction at a voltage $\hbar\omega/e$, or as a corresponding peak in d^2I/dV^2. Thus measurement of d^2I/dV^2 as a function of V gives the vibrational spectrum.

Tunnel junctions normally consist of crossed evaporated metal strips separated by a tunnelling barrier. For molecular spectroscopy the barrier is usually alumina, obtained by oxidising an aluminium bottom electrode in an oxygen glow discharge. Molecular species are incorporated by exposing the newly grown oxide to vapour or by applying dopant in liquid form. Fabrication is completed by evaporating a metal top electrode. Spectra are obtained from samples at 4.2 K by standard AC bridge techniques.

Mode *frequencies* of molecules embedded in tunnel junctions are surprisingly insensitive to changes in their local environment, produced, for example, by different top electrodes, and the small shifts that are observed, typically 1% are well understood (Adkins and Sleigh 1987). Kirtley and Hansma (1975, 1976) attributed changes in the position of benzoate and hydroxyl peaks to the interaction of oscillating dipoles, representing each mode, with electrical images in the top electrode. The magnitude of the interaction depends on the distance of the dipole from the image plane, which in turn is related to the metallic radius of atoms in the electrode.

0953-8984/89/061107 + 12 $02.50

By contrast IETS *intensities* change dramatically with different top electrodes or when the surface is roughened. Geiger *et al* (1969) showed that the intensities of hydrocarbon peaks for unknown dopants (obtained by exposing alumina surfaces to the atmosphere) were larger for Pb, Au and Ag than for Sn and In top electrodes. No molecular spectral structure was observed for Al or Mg top electrodes. The authors explained the results in terms of atomic size, with smaller atoms penetrating further into the alumina, but in order to obtain a monotonic correlation of intensity with size they had to assume arbitrary charge states when specifying ionic radii.

Roughened surfaces can be prepared by evaporating a layer of CaF_2 under the bottom Al electrode (Dragoset *et al* 1982, Varker *et al* 1983). The roughness of similarly prepared Al films has been estimated in surface plasmon studies (Endriz and Spicer 1971), and is believed to have an RMS height variation increasing from about 1 to 4 nm as the CaF_2 thickness is increased from 100 to 250 nm, with a correlation length in the plane of the film decreasing from 90 to 40 nm. Although these values depend on details of the preparation process, the thickness of CaF_2 provides a convenient measure of film roughness.

Varker *et al* (1983) showed that Al–Al_2O_3–Pb junctions doped with benzoate grown on substrates roughened with CaF_2, and hence with increased surface roughness, had weaker organic peaks than junctions grown on standard 'smooth' glass slides. Indeed, for fluoride thicknesses of 50 nm the dopant peaks were negligible, leaving a spectrum which appeared much like that of an undoped junction. The authors, therefore, speculated that the substrate roughening affected only modes at the alumina–metal interface, leaving the bulk barrier spectrum (such as the alumina peak at 117 meV) unaltered. A similar result was noted by Dragoset *et al* (1982), with p-chlorobenzoate as dopant, but only one thickness of CaF_2 was used.

A difficulty with all previous studies of top-electrode and roughening effects has been that even in the ideal smooth junction a detailed theoretical analysis of mode intensities has been impracticable, mainly because of the complexity of the dopant molecule. In this work, therefore, we investigated the effects of different top electrodes and of substrate roughening on the IET spectrum of a simple molecule, formic acid, which adheres to the alumina as the *formate ion*, a simple four-atom species. The free ion has six normal modes, which should be contrasted with the 36 modes of benzoate. A consequence is that the different formate modes are distinct and well understood, allowing the effects of local environment on different types of motion to be studied. Because of this inherent simplicity it is possible to identify the most important factors influencing the intensity, and hence to compare theoretical and experimental peak intensities (Sleigh *et al* 1986). The calculations follow the approaches of Kirtley *et al*

Table 1. Vibrational modes of the formate ion.

Normal mode	Designation	Energy (meV)
C–H stretch	$\nu_{C\text{-}H}$	358
C–H out-of-plane bend	$\pi_{C\text{-}H}$	131
C–H in-plane bend	$\rho_{C\text{-}H}$	172
CO_2 asymmetric stretch	$\nu_{asC\text{-}O}$	200
CO_2 symmetric stretch	$\nu_{sC\text{-}O}$	166
CO_2 scissors stretch	δ_{OCO}	~90
Ionic rock	—	20–50

(1976) and Phillips and Adkins (1985), associating a partial charge with each atom and calculating the contributions to the conductance that arise from the interaction between tunnelling electrons and the oscillating partial charges treated as dipoles. In this paper we extend the analysis to account for variation in *relative* peak intensity with top electrode. However, to explain changes in *absolute* intensity and the observed reductions in organic peak intensity with roughened substrates we propose a more detailed model for the interface in which the organic layer (but not the alumina) may be penetrated by atoms of the top electrode.

2. Experiment

Vapour-doped formate tunnel junctions were fabricated as described earlier (Sleigh *et al* 1986) with the following top electrodes: Ag, Al, Au, Cu, In, Pb and Sn. Typical spectra are shown in figure 1 as $(1/\sigma_0)\,\mathrm{d}^2I/\mathrm{d}V^2$, the second derivative normalised to the zero-bias conductance, with the elastic background removed. The formate peaks are assigned in table 1 as in Sleigh *et al* (1986). It can be seen immediately from figure 1 that the top electrode has a marked effect on the intensity of the formate peaks, ranging from strong spectra with lead to virtually no dopant structure with aluminium. Although the precise ordering of peak intensity with metal differs from that of Geiger *et al* (1969), the general

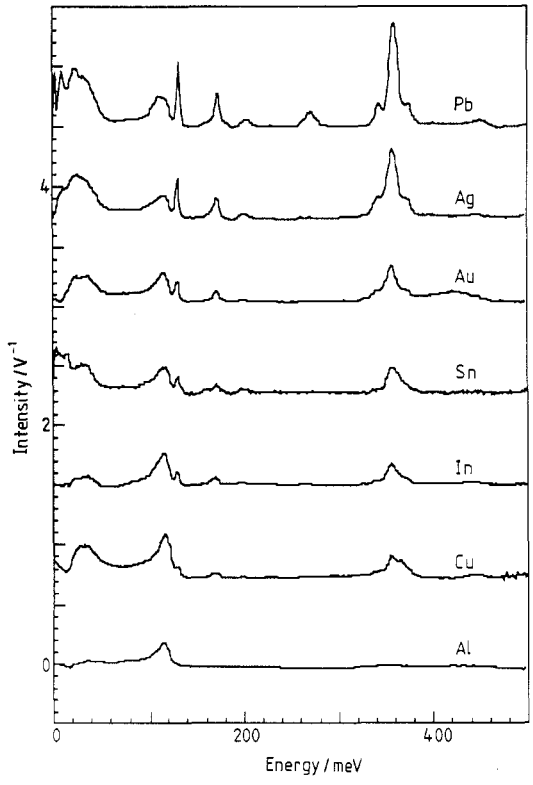

Figure 1. Typical spectra, plotted as $(1/\sigma_0)\,\partial^2 I/\partial V^2$ where σ_0 is the zero-bias conductance of formic acid (formate) with different top electrodes (zeros displaced).

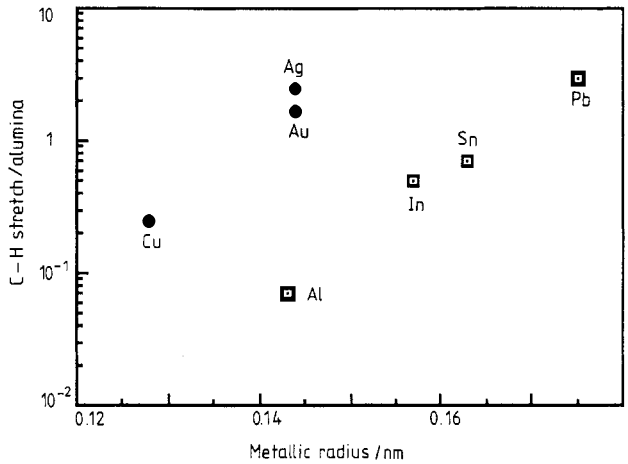

Figure 2. Intensities of the C–H stretching mode, normalised to the height of the alumina peak at 117 meV, plotted as a function of metallic radius.

trend is similar. Detailed analysis also shows that the *relative* heights of the C–H out-of-plane bend peak (at 131 meV) and the C–H stretch (at 358 meV) vary between samples with differing top electrodes (see figure 3, later).

Figure 2 shows the intensity of the C–H stretching mode, normalised to that of the Al_2O_3 peak at 117 meV, plotted logarithmically against *metallic* radius. (Because the Al_2O_3 peak has a constant intensity within the uncertainties of the calibration of absolute intensities, it is a convenient reference.) Metallic radii are directly relevant to the tunnelling problem because, to be considered part of the top electrode, the surface metal atoms must share delocalised electrons with the bulk metal. At first sight there is no obvious correlation between intensity and radius, but by dividing the metals into two classes, the noble metals on the one hand (full symbols) and groups III and IV metals on the other (open symbols), a consistent trend within each class of increasing intensity with increasing radius is obvious.

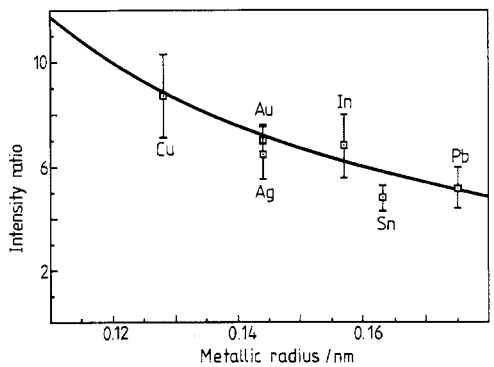

Figure 3. The ratio of the area under the C–H stretching-mode peak to that of the C–H out-of-plane bending mode peak plotted against metallic radius. The full curve is a theoretical fit calculated as described in the text with the position of the image plane chosen to give the best fit.

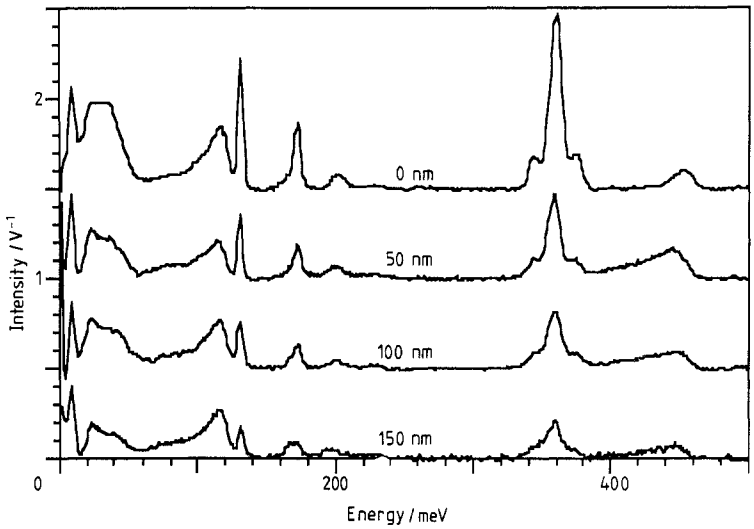

Figure 4. Typical spectra of formic acid with Pb–1% Bi top electrodes for a smooth substrate and for junctions prepared with prior deposition of CaF_2 films of different thicknesses. A similar trend is observed for pure Pb top electrodes.

The relative intensity of the C–H stretching mode (358 meV) to the C–H bend (131 meV) is shown in figure 3, again as a function of metallic radius. We note that the relative intensity of these peaks *decreases* with increasing atomic radius in a regular way for both groups of metals.

For the study of roughened barriers, junctions were prepared by evaporating different thicknesses of CaF_2 on the substrate before deposition of the aluminium base electrode. This was followed by plasma oxidation, doping and deposition of a top Pb or Pb–1% Bi electrode. It was noticeable that rougher junctions required a longer oxidation time to obtain similar junction resistances, although the height of the alumina peak at 117 meV in the spectra remained essentially constant (see figure 4). The most significant effect shown in figure 4 is the decrease in intensity of the formate peaks with increasing CaF_2 thicknesses. The general trend is the same as that seen by Varker *et al* (1983), although we find that spectra persist to greater thicknesses of CaF_2, a feature which we ascribe to our use of somewhat thicker films for the aluminium base electrode, and to different oxidation and doping procedures.

Figure 5 shows the intensity, normalised to the smooth junction, of each prominent peak in the spectrum as a function of CaF_2 thickness. Although there is relatively large uncertainty (up to 25%) associated with some points, peaks involving C–H motion appear to decrease in intensity more rapidly with roughness than those involving significant oxygen motion.

3. The model surface

In this section the variation in intensity of the formate peaks with metallic radius and roughness are explained in terms of a detailed model of the interface. Three distinct aspects are important: the structure of the bare alumina surface, packing of formate

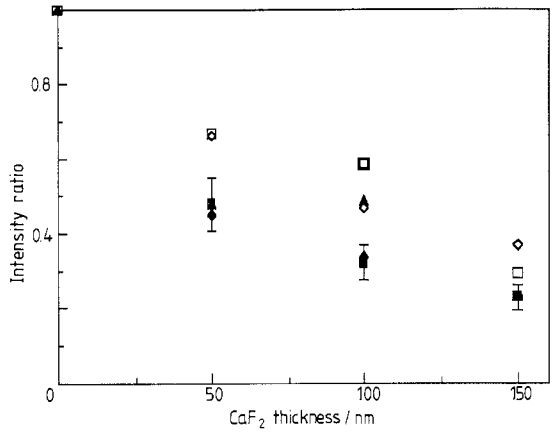

Figure 5. The intensities of different peaks in the spectra shown in figure 4, normalised to those of the smooth junction, plotted as a function of CaF_2 thickness. □, rocking; ◆, π_{C-H}; ▲, ρ_{C-H}; ◇, ν_{asC-O}; ■, ν_{C-H}.

ions on this surface and the structure of the top metal electrode. Although a detailed quantitative treatment of each of these aspects would present formidable problems, we believe that qualitative physical arguments are sufficient to develop a convincing model which explains the main experimental results.

3.1. The alumina surface

Crystalline alumina exists in a variety of forms, all of which can be represented as slightly distorted close-packed oxygen arrays with aluminium ions contained in tetrahedrally or octahedrally coordinated sites, a structure permitted by the small radius of the Al^{3+} ion (0.05 nm) in comparison with that of O^{2-} (0.13 nm) (Wells 1962). Different crystal structures correspond to different arrangements of the Al ions (Wells 1962). The *amorphous* form will almost certainly retain local close packing of oxygen ions with disorder introduced through the arrangement of the Al and through disruptions in the close packing. We expect that the *surface* of an amorphous alumina film may be represented in a similar way with Al ions randomly distributed in one-third of the available sites above the outer plane of close-packed oxygen ions. Because water is present during oxide growth and detected in the ITS of undoped junctions (as a peak at 450 meV), at least some of these surface Al ions will trap, and be neutralised by, hydroxyl ions.

On a *rough surface*, there must be steps in the oxygen planes. For example, with an RMS amplitude variation perpendicular to the plane of 4 nm and a correlation length in the plane of 40 nm, steps in the oxygen planes must occur every five atoms or so. Surface disorder, therefore, now not only reflects the disorder of the bulk alumina, but also contains additional roughness-induced disorder in the form of these steps.

3.2. Formate adsorption

Formic acid in adsorbed as formate ions with loss of surface hydroxyl groups as water. The separation of the oxygen atoms in the formate ions is 0.23 nm, which is only slightly

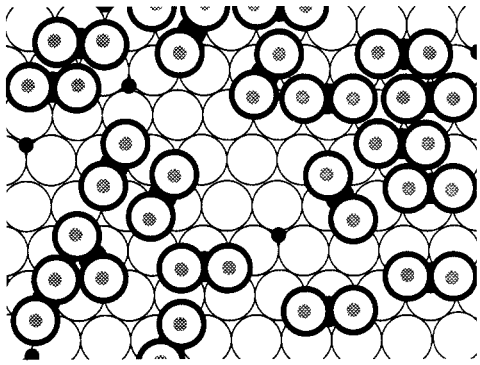

Figure 6. A model of formate ions on an alumina surface, showing an underlying close-packed sheet of oxygen ions (large open circles), the random arrangement of Al ions (small full circles) and formate oxygen atoms (large heavy circles). The Al ions that lie below each formate oxygen are shown hatched.

smaller than the oxygen–oxygen separation of 0.25 nm in a close-packed plane of oxygen ions in alumina. Formate ions can, therefore, pack on the alumina so that the formate oxygen ions form part of what would be the next close-packed plane. Assuming that, as far as possible, every formate oxygen atom sits above an Al ion in the surface, the maximum density of formate ions on the surface can be estimated to be approximately $6 \times 10^{18}\ m^{-2}$, which is in good agreement with the measured maximum coverages of $4 \times 10^{18}\ m^{-2}$ for formate and $7 \times 10^{18}\ m^{-2}$ for benzoate ions (Scholten *et al* 1965, Langan and Hansma 1975).

Figure 6 illustrates just such a random arrangement of formate ions on an alumina surface, in which each ion covers two of the randomly distributed Al ions. Inevitably there are holes in the packing, ranging from a minimum feret of approximately 0.16 nm, which occurs for an ordered arrangement of Al ions, to larger holes with decreasing statistical probability. Also, the observation of a hydroxyl peak in fully doped junctions suggests that some of the Al ions retain hydroxyl ions. Steps in the close packing will be expected, in general, to lead to less effective packing.

3.3. Metal–formate interface

The structure of the interface between the metal film forming the top electrode and the formate–alumina surface is governed by two distinct factors. At issue is the question of whether the metal follows the contour of the formate, making contact with alumina where holes are left in the packing, or whether it forms a planar film supported away from the alumina by the formate ions. The first factor is the relative magnitude of the free-surface energy of the metal and the energy of reaction between the metal and the alumina/formate. In order to penetrate the formate layer the surface area of the metal must increase, but energy is gained by reaction between the metal and the alumina/formate with which the metal makes contact. The second factor determining penetration is the size of the metal atoms because larger atoms may not be able to enter the holes between the formate ions.

The interfacial energetics are clearly related to the problem of wetting and adhesion, although even for that better defined problem there is little precise quantitative infor-

Table 2. Trends in top-electrode parameters. The magnitude of each parameter decreases from top to bottom.

Surface energy/atom	Reactivity	Metallic radius
Au	Al	Pb
Cu	Sn	Sn
Ag	In	In
Al	Pb	Ag
Sn	Cu	Au
In	Au	Al
Pb	Ag	Cu

mation for the case of interfacial energies between metals and refractory oxides (Stoneham 1982–3). However, two contributions may be distinguished. The first is a 'physical' interaction which does not involve electron transfer. This may be represented as deriving from a simple electrostatic interaction between the oxide ions and their electrical images in the metal surface. As pointed out by Stoneham (1982–3), for a given oxide this will be essentially the same for all metals. The second contribution to the interface energy is 'chemical', involving electron transfer, and this depends strongly on the metal. A useful measure of the relative importance of this chemical term is provided by Naidich (1981), who gives energies of reaction between various metals and alumina. According to this measure, the reactivity should increase in the order Ag, Au, Cu, Pb, In, Sn, Al. Similar ordering is also found by examining bond energies.

Precise quantitative analysis of our model is impossible in the absence of reliable

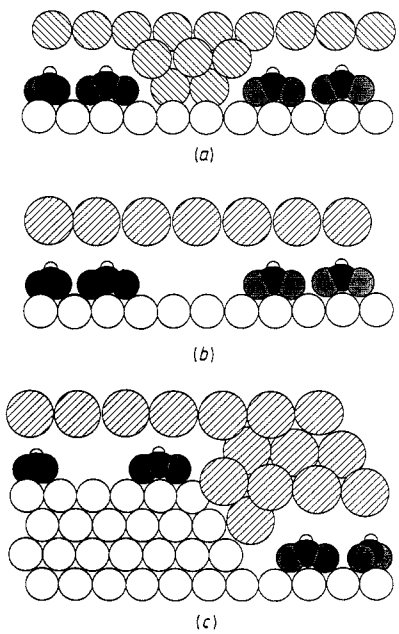

Figure 7. Schematic interfacial structures showing the forms of the top-electrode interface (*a*) for Sn, In, Cu; (*b*) for Ag, Au, Pb on smooth doped surfaces; and (*c*) for a Pb film on a roughened surface.

values for the quantities involved, but trends of the three relevant parameters are set out in table 2. Metals with small surface energies and large interfacial energies will tend to follow the contours of the formate layer, making contact with the alumina through spaces in the packing of formate ions (figure 7(*a*)), while metals with large surface energies, small interfacial energies or large size will tend to form a planar interface (figure 7(*b*)).

4. Discussion

4.1. Top-electrode effects

The discussion of the previous section suggests that the differences in observed spectra can be related to different structures of the oxide–formate–top-electrode interface. It is clear that in a structure of the form shown in figure 7(*a*) direct contact between metal and oxide reduces the average tunnelling path and bypasses the molecules. Because the tunnelling conductance is exponentially dependent on barrier thickness, even a small area of direct contact leads to a large reduction in the observed intensities of molecular spectra.

The magnitude of the effect can be estimated by extending an argument due to Cederberg (1981), originally proposed to explain the non-linear variation of IETS intensities with dopant coverage. The areas under the peaks in the inelastic spectra shown in figure 4 represent the change in the inelastic contribution to the conductance $\Delta\sigma$, normalised to the zero-bias conductance σ_0. For a doped junction of total area A_0 and with an area A_m of direct metal–oxide contact, weighting the different areas by the relative tunnelling probabilities gives

$$\frac{\Delta\sigma}{\sigma_0} = \frac{(A_0 - A_m)}{(A_0 - A_m) + A_m\, e^{2\alpha\delta}} \left(\frac{\Delta\sigma}{\sigma_0}\right)_0$$

where δ is the difference in the effective thickness of the tunnelling barrier for the contacting and non-contacting areas and $(\Delta\sigma/\sigma_0)_0$ is the strength of the spectral feature for no metal penetration. Notice that the effect of the area A_m is enhanced by the factor $e^{2\alpha\delta}$ representing the exponentially increased tunnelling probability. The factor R by which the intensity of a spectral line is reduced by the areas of contact may be written

$$R \equiv (\Delta\sigma/\sigma_0)/(\Delta\sigma/\sigma_0)_0 = (1 - s)/[1 + s(e^{2\alpha\delta} - 1)]$$

where $s = A_m/A_0$. Typically α^{-1} is 0.2 nm so that for $\delta = 0.5$ nm (the effective height of a formate ion), $e^{2\alpha\delta}$ is over 100. R is therefore approximately 0.5 for s less than 1%.

The results shown in figure 2 can be understood on the basis of this estimate and the trends shown in table 2. We expect Ag and Au to form a planar film supported above the layer of formate ions (figure 7(*b*)) because of their large surface energies and small reactivities. Sn and In make direct contact with alumina over a few per cent of the area through holes in the formate layer because of their smaller surface energy and larger reactivities. Cu will do the same because in spite of its large surface energy, its reactivity is larger than those of Au or Ag, and the radius is much smaller. Pb is in the opposite limit, where, although the energies are favourable, it is prevented from filling all but the largest holes in the statistical distribution by its large atomic size. Al is an extreme case because it wets alumina (Naidich 1981), and is also small, so that the absence of spectra may be a result of a much greater area of contact or because it displaces formate ions from the surface. (It should be noted that a single metal atom projecting from a close-

packed sheet is not sufficient to bridge the gap between metal and alumina, and several atoms are needed. Taking the distance of the formate H atom to the image plane as 0.2 nm (Sleigh *et al* 1986), the distance to the alumina oxygen ions is approximately 0.5 nm.)

The ideas developed above do not explain the differences in behaviour of different molecular modes and an explanation of the results shown in figure 3 requires a more detailed examination of other factors influencing the observed intensities in the contributing parts of the junction. The strength of coupling between a tunnelling electron and an oscillating dipole (representing a vibrating atom) depends critically on the position and orientation of the dipole with respect to the electrodes (Phillips and Adkins 1985). The field of a dipole parallel to the electrode is partly cancelled by that of the nearest image, while that of a dipole perpendicular to the electrode is enhanced. Because the C–H stretching mode involves large hydrogen displacements perpendicular to the interface, it dominates the spectrum, but the intensity of the bending mode, where the hydrogen moves parallel to the interface, is critically dependent on the distance a_H between the hydrogen atom and the image plane. Using calculations of intensities described in a previous paper (Sleigh *et al* 1986), we have determined the expected intensity ratio as a function of atomic size on the assumption that a_H is linearly related to the metal atomic radius r_m. For the theoretical curve, plotted as the full curve in figure 3, $a_H = r_m + \lambda$, where $\lambda = 15$ pm. This calculation gives a good fit to experiment, and is consistent with the work of Kirtley and Hansma (1975, 1976), who found that peak *positions* move with top electrode as if the image plane is closer for smaller atomic radius (see also Adkins and Sleigh 1987).

For completeness we should also discuss the possibility that screening of the interaction field of the oscillating dipoles by the metal intrusions could contribute to the observed loss in inelastic intensity. The interaction of the dipole field with the tunnelling electron involves an integration over the tunnelling barrier. It is clear from figure 7(*a*), without detailed analysis, that the metal intrusions will reduce the lateral extent of the dipole field, and hence reduce the inelastic intensity. Following Phillips and Adkins (1985) the matrix elements can be calculated for the case where the lateral size of the junction is smaller than the junction thickness. Such a calculation serves to provide an upper limit to the expected effect for hydrogen modes, the most heavily screened. For a junction of lateral dimension equal to the width of the barrier, the calculations give a reduction of about 30% in intensity, but more importantly they show that the C–H stretching mode will decrease in intensity by a larger factor than the C–H bending mode. This follows from the fact that in the latter case the dipole, together with its image, gives a quadrupole field which is less affected by the lateral cut-off than is the dipole field. Because these predictions are not observed experimentally, we conclude that the 'shorting' effect dominates.

4.2. Surface roughening

The results described in § 2 show that roughening of a doped tunnel junction by means of a CaF_2 underlayer has no effect on barrier (alumina) modes but leads to a decrease in intensity of dopant (formate) modes as the CaF_2 thickness is increased. All three C–H modes (open symbols) behave in the same way, confirming the view of Varker *et al* (1983) that the decrease in spectral intensity does not arise from a roughness-induced change in the orientation of the absorbed molecule: any change in orientation would be expected to increase the intensity of the C–H out-of-plane bending mode and to decrease that of the stretching mode. The results also indicate that these modes, dominated by

hydrogen motion, decrease in intensity slightly more rapidly than do those involving oxygen.

There is, therefore, a striking similarity between intensity losses attributed to surface roughness and those due to top-electrode effects, suggesting a common mechanism based on penetration of the organic layer by the top electrode. The discussion of § 3 demonstrated the importance of the large atomic radius of Pb in preventing contact with the alumina, in spite of the favourable balance between interfacial and surface energies, so that good spectra are obtained with smooth junctions. Roughening of the substrate leads to an increased number of steps in both the oxide surface and the Pb film at the interface. The presence of steps is likely to make alumina more accessible to metal atoms. This can be seen from figure 6 if it is assumed that the effect of a step is to introduce a line on the surface which no formate ions may straddle. The interface can then be represented as in figure 7(*c*), where the lead film now makes more contacts with the alumina as a result of the presence of the roughness-induced steps. It should be borne in mind from § 4.1. that an effective area of only a few per cent is necessary to reduce the intensity of the spectrum by a factor of two, so that this model is consistent with the observation that the surface concentration of formate molecules is essentially unchanged with roughening (Varker *et al* 1983).

At first sight tunnelling might be expected to occur preferentially through the lower RHS in figure 7(*c*), but of course the oxide topography follows that of the underlying Al bottom electrode so that the oxide thickness is the same on both sides of the step. A step such as that shown will, however, give a small local area of barrier with a smaller effective thickness even in the undoped junction, thereby providing a natural explanation for the fact that roughened junctions require longer oxidation to produce the same resistance.

The model also explains two other experimental observations. Firstly, modes involving motion of the ion closest to the metal electrode will be more effectively short-circuited by metallic penetration to the oxide than those involving motion close to the alumina, where some residual interaction with the tunnelling electrons will occur. In the formate ion this means that C–H mode intensities decrease more rapidly with roughening than those involving oxygen, as seen in figure 5. Secondly, increased penetration of the formate on roughened substrates leads to a lower junction resistance. The trend of increased oxidation times, to produce the same junction resistance, with increased CaF_2 thicknesses should therefore be more pronounced in doped junctions. This is what is observed.

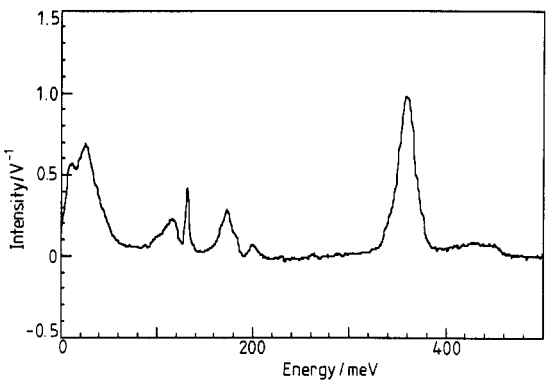

Figure 8. The spectrum of a roughened formate-doped junction with a Ag top electrode. The thickness of the CaF_2 underlayer was 150 nm.

Hitherto, all experiments on roughened junctions have used Pb top electrodes, but an extension of the argument to noble metals implies markedly different behaviour. Because we believe Ag and Au are prevented from making contact not by steric factors but because the metal–vacuum surface energy is much larger than the metal–alumina interfacial energy, roughening the surface should not lead to such a large reduction in mode intensities. In both smooth and rough junctions the films will tend to remain supported away from the alumina. To test this prediction a roughened junction was prepared using Ag as the top electrode: the results are shown in figure 8. Whereas for Pb the effect of 150 nm of CaF_2 is to reduce mode intensities by a factor of five, for a Ag top electrode the intensity is unchanged. This result provides strong experimental support for the model.

5. Conclusions

In this paper we have shown that the effects of different top electrodes and of surface roughness on the spectra of formate-doped tunnel junctions can be accounted for in terms of penetration of metal through the organic layer. The likelihood of penetration is increased if the atom has a large energy of interaction with alumina and a small metallic radius, but is decreased by a large metal–vacuum surface energy and large size. Ag, Au and Pb do not penetrate significantly, but Cu, Sn and In do. Al is an extreme case as regards reactivity because, of the metals considered, it alone wets alumina. The dominant effect of roughening is to reduce the importance of atomic size, so that Pb is able to 'penetrate' a formate layer on a rough surface, although Ag does not because its surface energy is large and its reactivity with alumina small. In all cases, the proportion of the total surface affected by penetration is small, the simple model showing that intensities are reduced by a factor of two when only 1% of the alumina is in direct contact with the metal of the top electrode.

References

Adkins C J and Phillips W A 1985 *J. Phys. C: Solid State Phys.* **18** 1313
Adkins C J and Sleigh A K 1987 *J. Phys. C: Solid State Phys.* **20** 4307
Cederberg A A 1981 *Surf. Sci.* **103** 148
Dragoset R A, Phillips E S and Coleman R V 1982 *Phys. Rev.* B **26** 5333
Endriz J G and Spicer W E 1971 *Phys. Rev.* B **4** 4144
Geiger A L, Chandrasekhar B S and Adler J G 1969 *Phys. Rev.* **188** 1130
Hansma P K 1982 *Tunnelling Spectroscopy: Capabilities, Applications and New Techniques* (New York: Plenum)
Kirtley J R and Hansma P K 1975 *Phys. Rev.* B **12** 531
—— 1976 *Phys. Rev.* B **13** 2910
Kirtley J R, Scalapino D J and Hansma P K 1976 *Phys. Rev.* B **14** 3177
Langen J D and Hansma P K 1975 *Surf. Sci.* **52** 211
Naidich J V 1981 *Proc. Surf. Memb. Sci.* **14** 354
Phillips W A and Adkins C J 1985 *Phil. Mag.* B **52** 739
Scholten J J F, Mars P, Menon P G and von Hardveld R 1965 *Proc. 3rd Int. Congr. on Catalysis* ed. W M H Sachter, G C A Schuit and P Zwietering (Amsterdam: North-Holland) p 881
Sleigh A K, Phillips W A, Adkins C J and Taylor M E 1986 *J. Phys. C: Solid State Phys.* **19** 6645
Stoneham A M 1982–3 *Appl. Surf. Sci.* **14** 249
Varker P R, Kirtley J R and Tsang J C 1983 *Solid State Commun.* **45** 417
Wells A F (ed.) 1962 *Structural Inorganic Chemistry* (Oxford: OUP)